



#### **OPEN ACCESS**

EDITED BY
Elizabeth Secord,
Wayne State University, United States

REVIEWED BY
Alessandro Mauro Spinelli,
Center for Rare Diseases & MetabERN
Coordinating Center, Italy
Alberto Olaya Vargas,

National Institute of Pediatrics, Mexico

\*CORRESPONDENCE

RECEIVED 19 June 2025
ACCEPTED 28 October 2025
PUBLISHED 20 November 2025

#### CITATION

Léon-Lara X, Ravens S, von Hardenberg S, Auber B, Bergmann AK, Ospina L, Guthmann F, Wübbena C, Brechler J, Weidemann J and Richter MF (2025) Low lymphozyte pool, colon perforation and hydrocephalus as clinical features in an infant with a postzygotic *PIK3CA* variant. Front. Pediatr. 13:1650077. doi: 10.3389/fped.2025.1650077

#### COPYRIGHT

© 2025 Léon-Lara, Ravens, von Hardenberg, Auber, Bergmann, Ospina, Guthmann, Wübbena, Brechler, Weidemann and Richter. This is an open-access article distributed under the terms of the Creative Commons Attribution License (CC BY). The use, distribution or reproduction in other forums is permitted, provided the original author(s) and the copyright owner(s) are credited and that the original publication in this journal is cited, in accordance with accepted academic practice. No use, distribution or reproduction is permitted which does not comply with these terms.

# Low lymphozyte pool, colon perforation and hydrocephalus as clinical features in an infant with a postzygotic *PIK3CA* variant

Ximena Léon-Lara<sup>1</sup>, Sarina Ravens<sup>1,2</sup>, Sandra von Hardenberg<sup>3</sup>, Bernd Auber<sup>3</sup>, Anke K. Bergmann<sup>3,4</sup>, Laura Ospina<sup>1</sup>, Florian Guthmann<sup>5</sup>, Christiane Wübbena<sup>6</sup>, Jan Brechler<sup>7</sup>, Jürgen Weidemann<sup>8</sup> and Manuela F. Richter<sup>5\*</sup>

<sup>1</sup>Institute of Immunology, Hannover Medical School, Hannover, Germany, <sup>2</sup>Cluster of Excellence RESIST (EXC 2155), Hannover Medical School, Hannover, Germany, <sup>3</sup>Department of Human Genetics, Hannover Medical School, Hannover, Germany, <sup>4</sup>Clinical Genetics and Genomic Medicine, University Hospital Würzburg, Würzburg, Germany, <sup>5</sup>Department of Neonatology, AUF DER BULT- Children's and Youth Hospital, Hannover, Germany, <sup>6</sup>Department of Pediatric Neurology, AUF DER BULT- Children's and Youth Hospital, Hannover, Germany, <sup>7</sup>Department of Pediatric Surgery, AUF DER BULT- Children's and Youth Hospital, Hannover, Germany, <sup>8</sup>Department of Pediatric Radiology, AUF DER BULT- Children's and Youth Hospital, Hannover, Germany

Pathogenic variants in the PIK3CA gene, which encodes the p110- $\alpha$  catalytic subunit of the phosphoinositide 3-kinase (PI3K), are commonly associated with overgrowth syndromes and cancer. We report a patient with the point variant c.1030G>A p.(Val344Met) in the PIK3CA gene who presented shortly after birth with viral sepsis and and severe lymphopenia, followed by colonic perforations. Histopathology showed ulcerative necrotizing colitis with lymphatic vascular malformation. The patient subsequently developed hydrocephalus requiring a ventriculoperitoneal shunt, complicated by refractory ascites that resolved with acetazolamide therapy. Awareness of the potential disease spectrum through early molecular diagnosis, combined with immunologic evaluation, comprehensive enabled management via closer clinical monitoring and timely interventions to prevent and control neurological and infectious complications. This case highlights the phenotypic heterogeneity of PIK3CA pathogenic variants and the importance of early precision medicine in pediatric care.

### KEYWORDS

PIK3CA gene mutation, severe lymphopenia, intern hydrocephalus, intestinal vascular malformation, necrotizing enterocolitis (NEC)

## Introduction

The PIK3CA gene encodes the p110- $\alpha$  catalytic subunit of the class I phosphoinositide 3-kinase (PIK), a key enzyme involved in numerous cellular processes, including cell growth, proliferation, survival, metabolism, and angiogenesis (1, 2). Class I PI3Ks promote the phosphorylation of phosphatidylinositol-(4,5)-bisphosphate (PIP2) to phosphatidylinositol-(3,4,5)-triphosphate (PIP3), thereby activating the PIK/AKT/mTOR signaling pathway (2, 3). Somatic variants in the PIK3CA gene are among the most prevalent genetic alterations in various human

cancers, including breast, colorectal, and cervical cancers, playing a critical role in oncogenesis (1, 2). Beyond cancer, *PIK3CA* variants are associated with a range of rare, non-malignant overgrowth disorders collectively known as PIK3CA-related overgrowth spectrum (PROS) (4, 5). These nonhereditary conditions are caused by postzygotic, somatic variants in the *PIK3CA* gene, which result in a mosaic distribution of affected tissues (4, 6). These variants lead to constitutive activation of the PIK/AKT/mTOR signaling pathway, promoting dysregulated cellular growth and proliferation (3).

The somatic nature of these variants contributes to the variability in phenotypic presentation, which also depends on the timing and location of the variant during development (3, 6). The PROS spectrum ranges from isolated, localized, or segmental overgrowth to syndromic disorders, including the megalencephaly-capillary malformation (MCAP) and megalencephaly-polymicrogyria-polydactyly-hydrocephalus (MPPH) syndromes (4, 7). Immune dysfunction is rarely reported in PROS, most often in association with lymphatic abnormalities (8). Timely diagnosis of PIK3CA-related disorders and associated complications is essential, given the progressive nature of overgrowth and potential complications (5, 6). Here, we present the clinical course of an infant with a de novo postzygotic c.1030G>A p.(Val344Met) variant. The infant initially presented with rotavirus-induced neonatal sepsis, complicated with transient immune dysregulation that lasted several weeks. During followup, he developed hydrocephalus requiring a ventriculoperitoneal (VP) shunt, which was complicated by refractory ascites, as well as an intraspinal peripheral nerve sheath tumor.

## Results

## Clinical presentation

A male infant was spontaneously delivered at 37 + 3 weeks of gestation in good general condition (Apgar 9/10/10), with a weight of 2,820 g (20th percentile), and a length of 52 cm (73rd percentile). Delivery occurred seven days after rupture of membranes, with clear amniotic fluid. Pregnancy (gravida 3, para 2) was uncomplicated, except for borderline abnormal fetal and umbilical Doppler findings two weeks before delivery. On examination, macrocephaly (head circumference 38 cm, >99th percentile), hypospadias, and right foot hexadactyly were noted. There was no family history of genetic or neurological diseases.

At 12 h of life, the infant was admitted to the NICU with suspected sepsis. He presented with poor general condition, hypothermia, hypoglycemia, mildly elevated IL-6 [81 pg/ml, (0–50)], and normal initial CRP concentration [0.82 mg/dl, (0–1.0)] (Figures 1A–C). Serial blood cultures at diagnosis were negative, while stool PCR was positive for rotavirus. A sharp rise in the inflammatory markers (IL-6 284 pg/ml and CRP 10.41 mg/dl) prompted broad-spectrum antibiotics (Figure 1D). Respiratory adaptation disorder initially required CPAP, followed by invasive ventilation after colonic perforations on days 8 and 11 (Figure 1A). Surgery revealed an extensive gangrenous

perforation involving the transverse and descending colon, requiring partial resection of the transverse colon and creation of an ostomy. Three days later, a second perforation in the transverse colon was treated with a protective terminal ileostomy. Histopathology showed patchy ulcerative necrotizing colitis with a mixed capillary-lymphatic vascular malformation. During hospitalization, the infant required prolonged parenteral nutrition, which caused transient severe cholestasis (Figure 1A). Initial neurological evaluation (EEG, cranial ultrasound, MRI) was unremarkable (Figure 2A).

Ultra-rapid whole genome sequencing (urWGS) identified a *de novo* postzygotic point variant, c.1030G>A, in exon 5 of the *PIK3CA* gene (NM\_006218.3). This variant results in a p.(Val344Met) amino acid substitution in the helical domain of the PI3K p110- $\alpha$  subunit and has been previously associated with PROS (6, 9–11). The same variant was also detected by panel sequencing of the resected intestine at a similar allele frequency (48.67% and 47.12%) as in the blood.

# Long-lasting lymphopenia during initial hospitalization

The infant exhibited persistent lymphopenia (Figure 3A) with markedly reduced B (CD19<sup>+</sup>) and T (CD3<sup>+</sup>) cells compared to neonates with sepsis (Figure 3B). Despite the overall reduction in the T cell pool, the proportions of CD8<sup>+</sup>, CD4<sup>+</sup>, and  $\gamma\delta$  T cells within the CD3<sup>+</sup> population were preserved, with a discrete increase in Treg cells (Figures 3C,D). Lymphocyte frequencies normalized after the initial hospitalization (Figure 3B), suggesting a transient alteration of the immune response to acute infection-related stress.

On day 10 of hospitalization, during colonic perforation, both pro-inflammatory (IL-6, CXCL-10, IFN- $\gamma$ ) and anti-inflammatory cytokines were elevated (Figure 4A). Meanwhile, CD4<sup>+</sup> and CD8<sup>+</sup> T cell functionality remained preserved, with expression of activation markers (CD69 and CD25) and TNF- $\alpha$  production following anti-CD3/anti-CD28 stimulation comparable to controls (Figure 4B). Monocyte frequency (CD14+) increased (Figure 4C) with a shift from classical inflammatory (CD14<sup>+</sup> CD16<sup>-</sup>) to non-classical anti-inflammatory (CD14<sup>+</sup> CD16<sup>+</sup>) phenotypes during hospitalization (Figure 4D).

# Follow-up of further complications and neurological involvement

At five months of age, the EEG showed intermittent frontal delta activity and isolated sharp waves, without seizures or infantile spasms. While growth was age-appropriate (Figure 5A), head circumference remained percentile-volatile (Figure 5B). By six months, cranial ultrasound revealed progressive hydrocephalus with enlargement of ventricles I-III, which was confirmed by MRI (Figure 2B). The MRI included a high-resolution, flow-sensitive, thin-slice T2 SPACE sequence, showing an anatomically patent aqueduct and

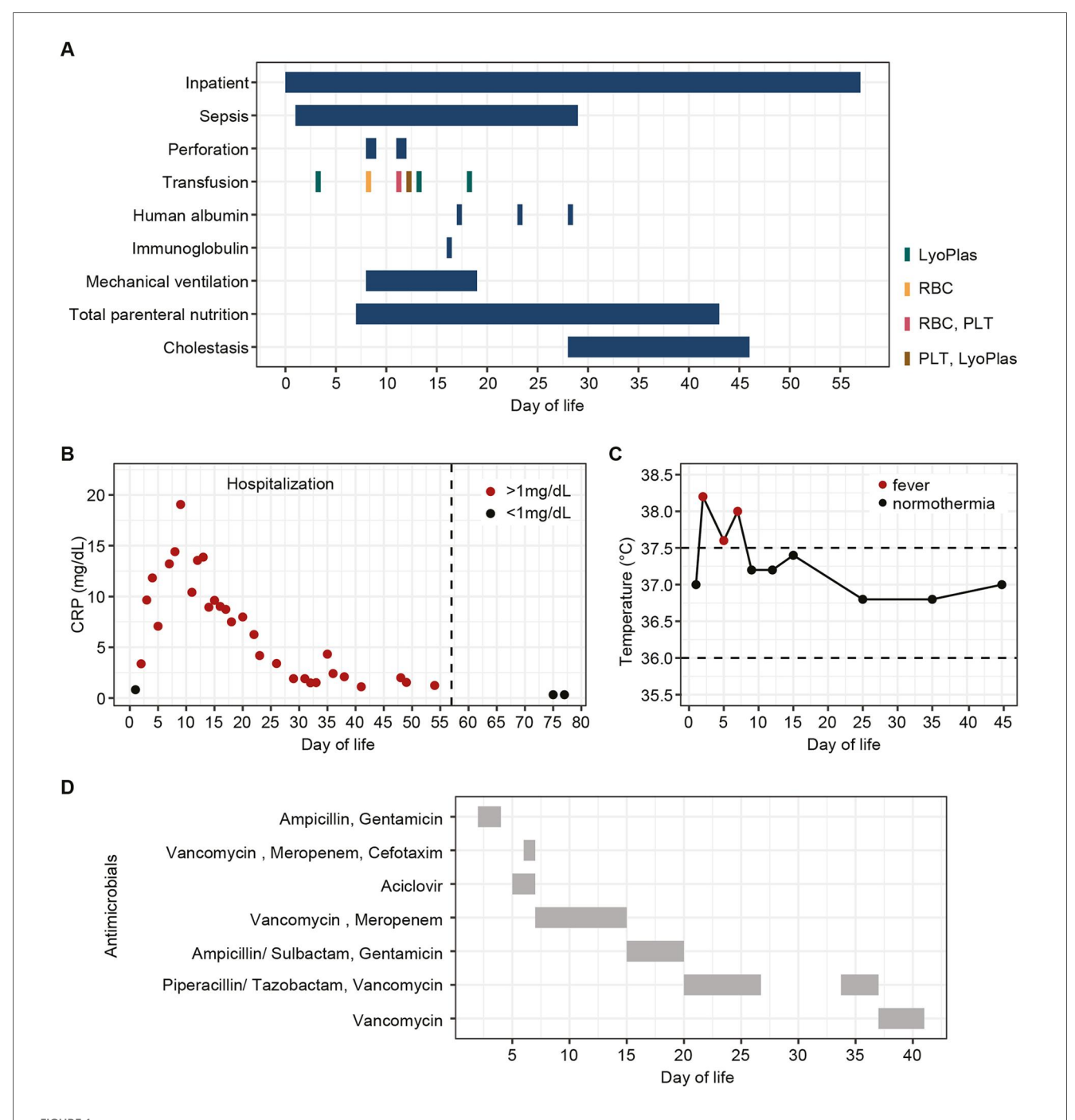


FIGURE 1 Clinical course and management during initial hospitalization. (A) Schematic overview of complications and interventions by day of life. (B) C-reactive protein (CRP) levels by day of life, >1 mg/dl (red dots), were considered elevated. (C) Body temperatures by day of life; values >37.5°C (red dots) were considered fever. (D) Antibiotic and antiviral treatments during hospitalization by day of life. LyoPlas, lyophilized plasma; RBC, red blood cells; PLT, platelets.

visible CSF flow phenomena. A VP shunt was placed at seven months; however, by 12 months, the patient developed refractory ascites. Serial cerebrospinal fluid (CSF) removal and abdominal punctures were required due to ongoing CSF overproduction (Figure 2C). CSF analysis showed markedly elevated albumin levels [2,520 mg/L, (120–240)], indicating pronounced barrier dysfunction. As an incidental finding during follow-up, a 6 mm diameter benign intraspinal tumor

of the nerve roots at the L3/L4 level was detected, with stable size on subsequent evaluations (Figure 2D). From 13 months of age, an off-label therapy trial with acetazolamide significantly reduced CSF and ascites volumes, facilitating motor development. By 15 months, the child achieved independent walking with only mild motor delay. He feeds orally, vocalizes, and performs small tasks. Long-term development outcomes remain to be determined.

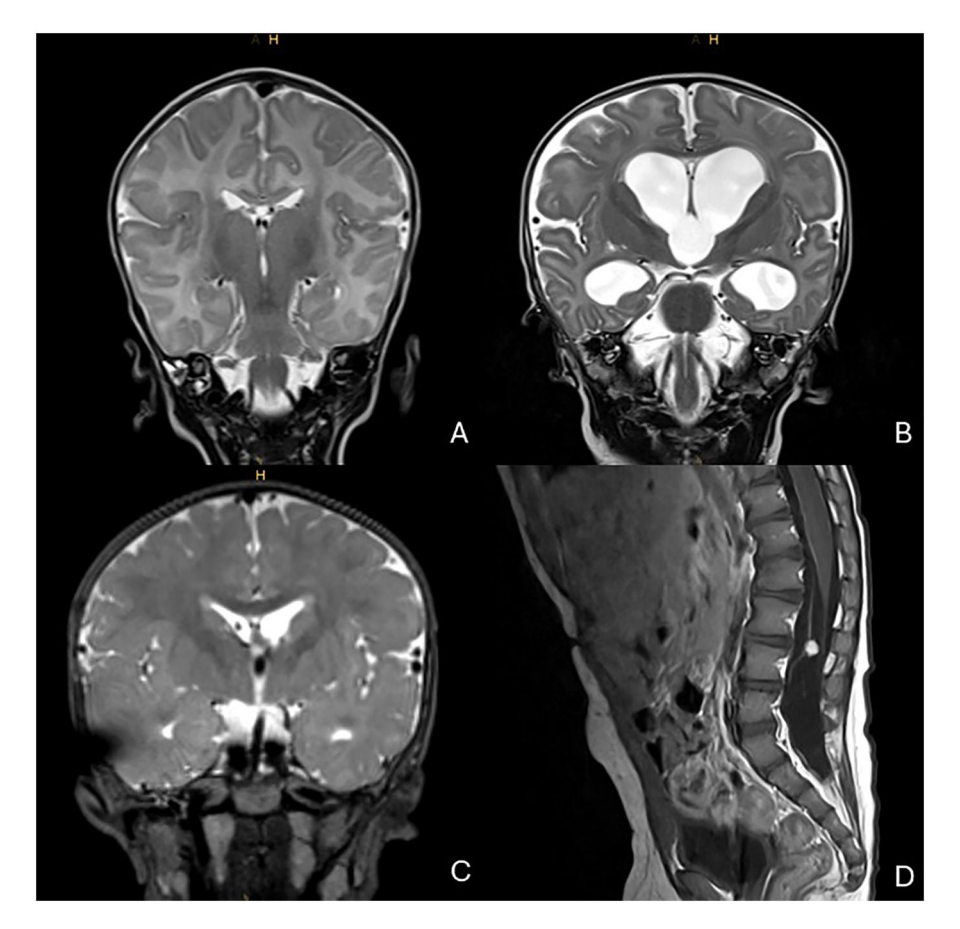


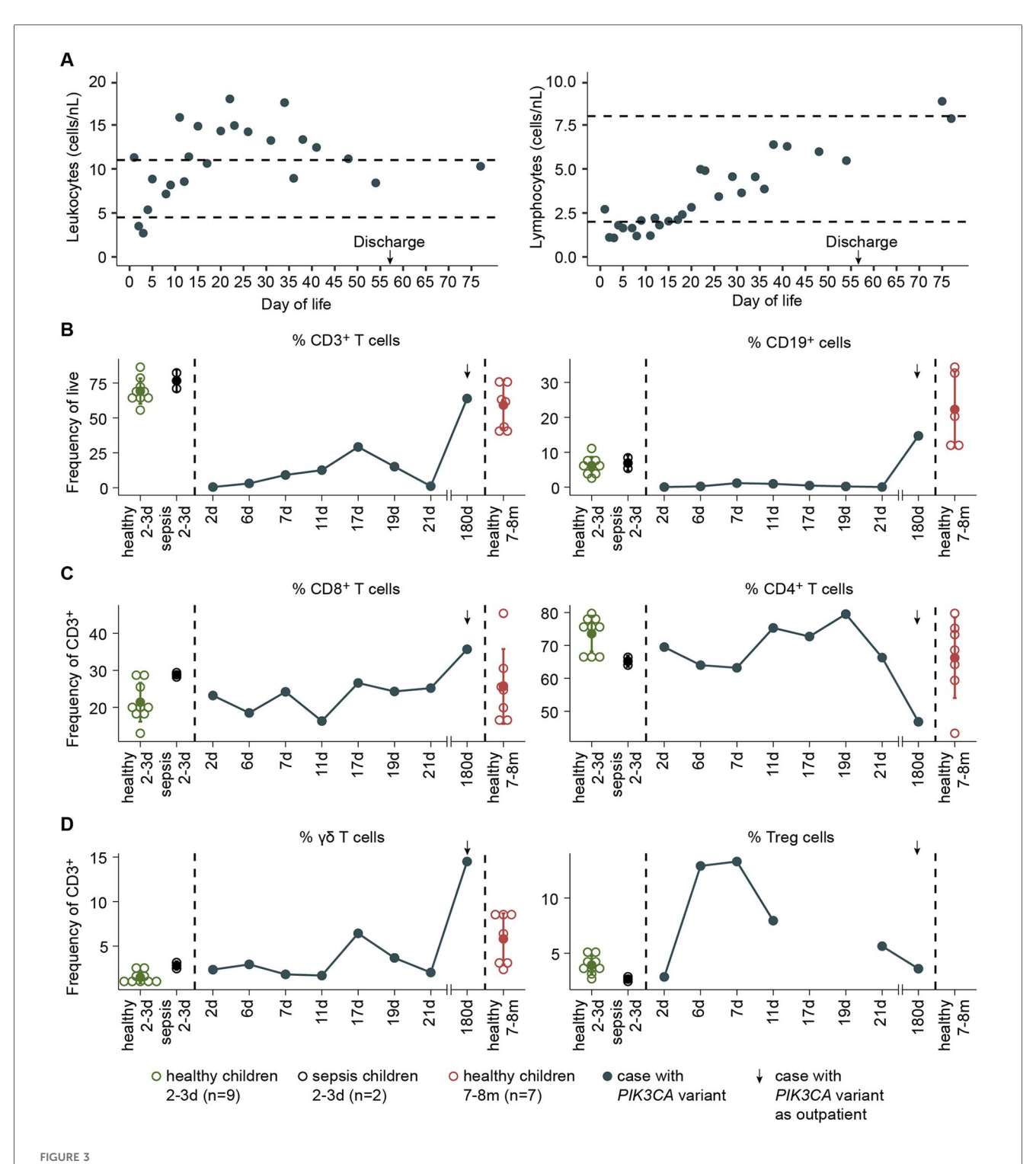
FIGURE 2
MRI imaging over time. (A) T2-weighted MRI during initial hospitalization (1 month, 17 days of age); normal cerebral ventricular width. (B) T2-weighted MRI at 6 months, 18 days of age; hydrocephalus with enlargement of ventricles I–III. (C) T2-weighted MRI at 1 year, 24 days of age; relief of hydrocephalus via right frontal shunt catheter. (D) T1-weighted MRI with contrast at 1 year, 10 months of age; solid nodule with contrast enhancement, stable in size since initial detection at 1 year, 24 days of age.

## Discussion

Pathogenic PIK3CA variants are commonly associated with oncogenesis, overgrowth, and vascular malformations (3, 6). Dysregulated PI3K signaling can also contribute to immune dysfunction, including infection susceptibility and autoimmune manifestations (12). While immunodeficiency is well described in PIK3CD variants (12), immune dysregulation has not been previously reported in PROS (6, 11). Here, we present a patient with a pathogenic PIK3CA variant who developed prolonged severe neonatal lymphopenia in the context of viral sepsis and peritonitis. The early atypical viral infection, followed by severe peritonitis, may have triggered a transient state of immune dysfunction that resolved once the septic episode subsided. Nevertheless, since PI3K signaling plays a central role in cell proliferation (1, 2, 12), constitutive activation due to the PIK3CA variant may have contributed to the lymphopenia and the clinical complications observed. Early detection of the variant through molecular diagnostics, combined with immune monitoring, was crucial for contextualizing, interpreting, and managing these complications. As no further severe infections

have occurred, long-term disease progression remains to be determined. Features resembling atypical necrotizing enterocolitis (NEC) were observed in our patient, with histopathology revealing ulcerative necrotizing colitis and a lymphatic vascular malformation. This represents the second reported case of such a presentation in PROS (13), highlighting that, in the neonatal period, PROS can manifest with gastrointestinal disease mimicking atypical NEC, most likely related to the intestinal vascular malformation.

The c.1030G>A p.(Val344Met) variant has been associated with MCAP (9, 10). In this case, macrocephaly was primarily caused by CFS overproduction. Acetazolamide therapy effectively reduced CSF secretion and improved neurologic outcome, highlighting its value when VP shunt treatment is insufficient. Targeted therapies, including PIK inhibitors (e.g., alpelisib) and mTOR inhibitors (e.g., sirolimus), are promising options in PROS by controlling disease progression and improving organ dysfunction (14–16). However, such therapies should be used with caution, particularly in patients with infection susceptibility, given the central role of PI3K in immune signaling (17).



Lymphocyte profile in a patient with PI3KCA pathogenic variant. (A) Leukocyte and lymphocyte counts by day of life. (B) Frequency of CD3T cells and CD19+ cells among live PBMCs from the patient (blue), healthy neonates at 2–3 days (green), neonates with sepsis at 2–3 days (black), and healthy infants at 7–8 months (red). (C) Frequency of CD8T cells, CD4T cells, (D)  $\gamma\delta$  T cells, and Treg cells among CD3T cells of the indicated donors.

In conclusion, this case expands the phenotypic spectrum of *PIK3CA* pathogenic variants and underscores the importance of multidisciplinary monitoring and careful neurological surveillance. Individualized treatment, including pharmacological

CSF reduction and consideration of targeted therapies, may improve outcomes. Further research is needed to clarify the relationship between *PIK3CA* variants and immune dysregulation to guide the safe application of targeted therapies.

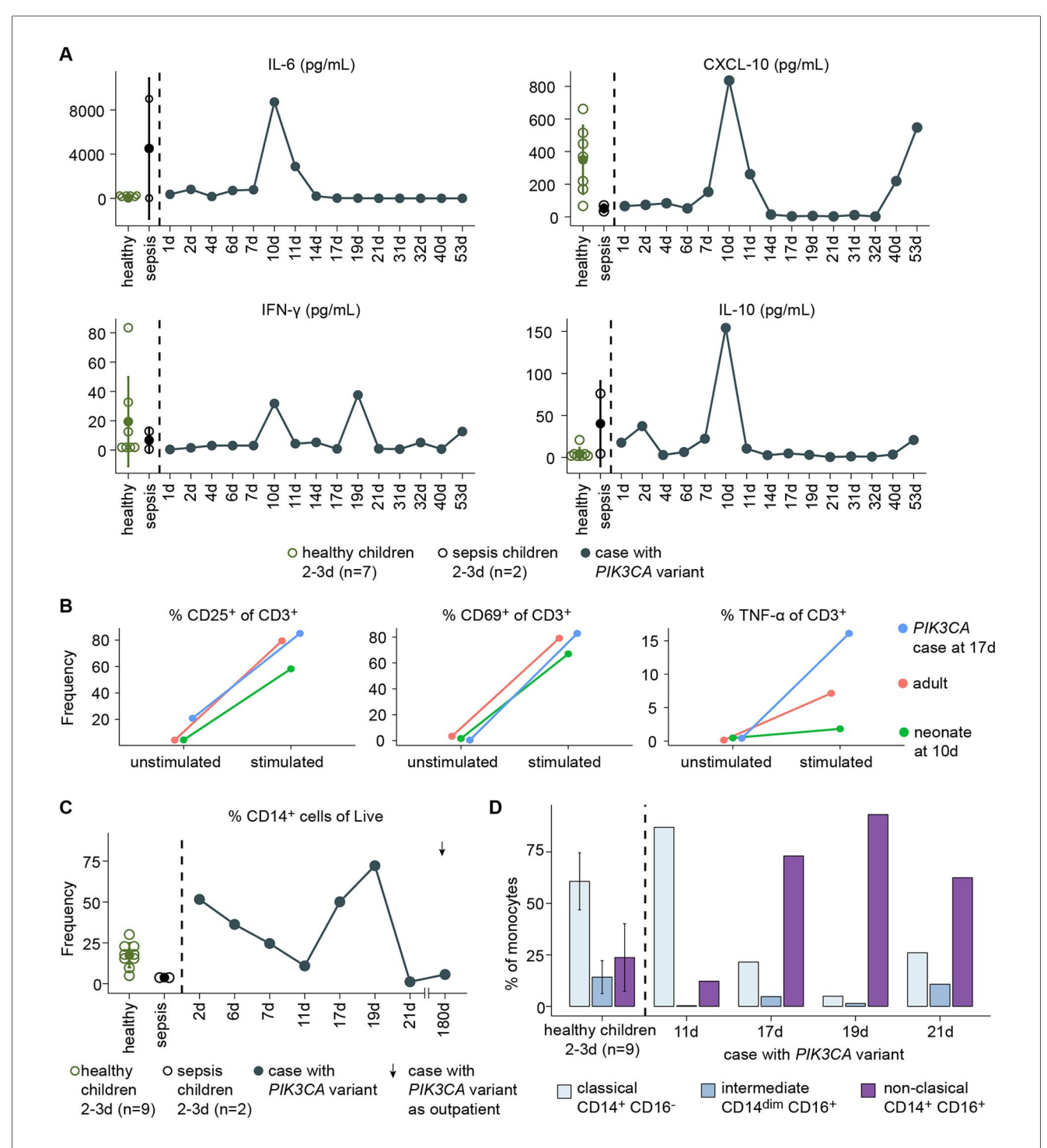
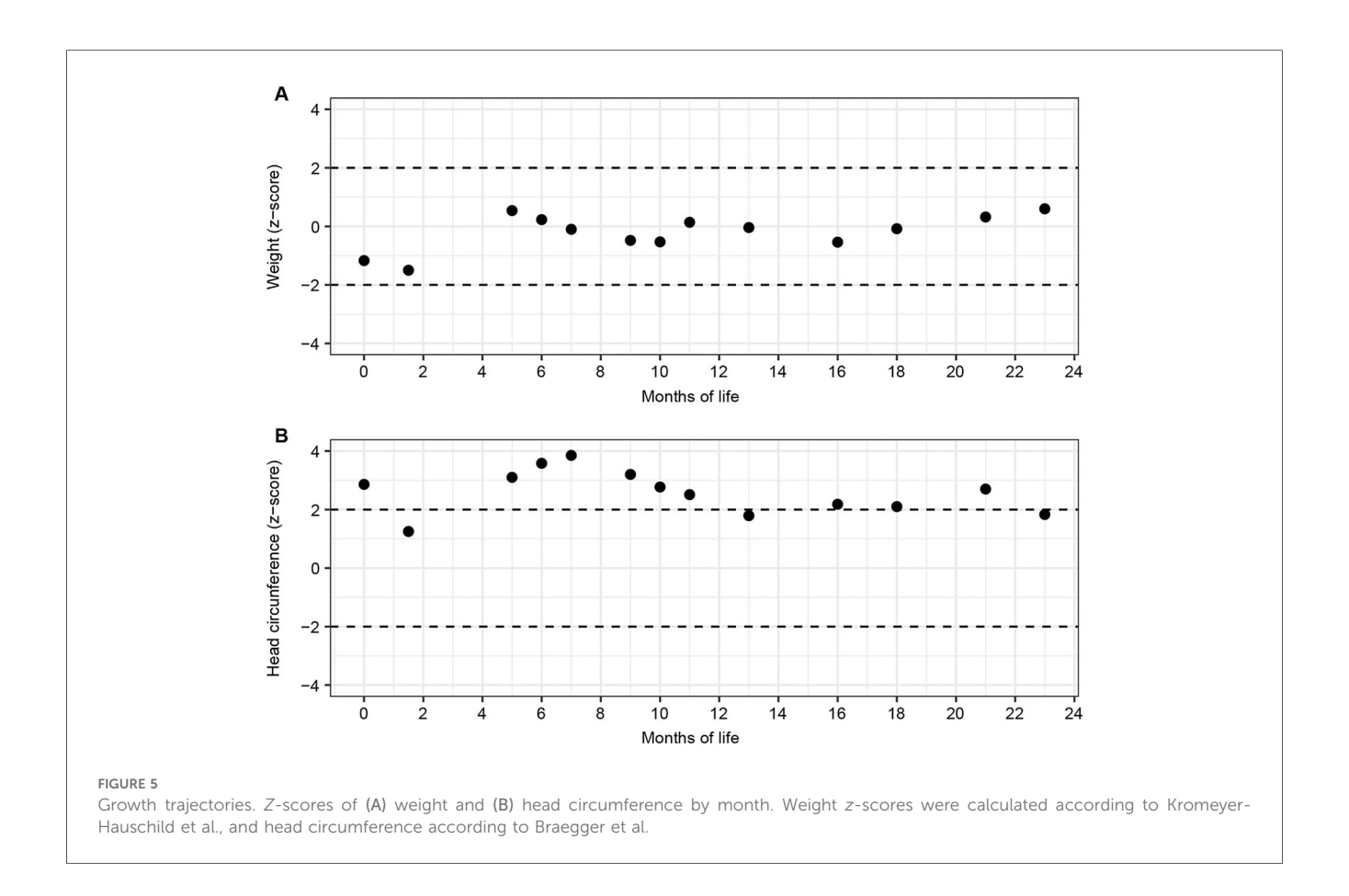


FIGURE 4 Immune profiling in a patient with *PI3KCA* pathogenic variant. (A) Plasma cytokine levels in the patient (blue), healthy neonates at 2–3 days (green), and neonates with sepsis at 2–3 days (black). (B) Frequency of CD25, CD69, or TNF- $\alpha$  among CD3T cells following anti-CD3/anti-CD28 stimulation in the patient at 17 days of age (blue), a healthy adult (pink), and a healthy neonate at 10 days of age (green). (C) Frequency of monocytes (CD14+) among live PBMCs in the patient (blue), healthy neonates at 2–3 days (green), and neonates with sepsis at 2–3 days (black). (D) Immunophenotype of CD14+ cells of the patient and healthy neonates at 2–3 days of age.



# **Methods**

## Ultra-rapid genome sequencing

EDTA blood was processed using the Illumina DNA PCR-Free Library Preparation Tagmentation Kit, followed by whole genome sequencing (WGS) on an Illumina NovaSeq 6000 sequencer. Sequencing reads were aligned to the human reference genome GRCh38. TruSight<sup>TM</sup> Software (Illumina, Suite v2.6) and centerspecific bioinformatics pipeline were used for alignment, variant calling, variant annotation, filtering, and curation. In addition to variant allele frequency data, prediction tools including phyloP, SIFT, PolyPhen-2, FATHMM, CADD, and REVEL were used. Furthermore, LOVD (https://databases.lovd.nl/shared/), ClinVar (https://www.ncbi.nlm.nih.gov/clinvar), and gnomAD (https://gnomad.broadinstitute.org/) were screened for reported entries of the identified variant. Variant interpretation followed the standards and guidelines of the American College of Medical Genetics and Genomics (18).

## **Ethics**

Inclusion and sample collection were conducted in accordance with the Declaration of Helsinki and approved by the Institutional Review Board of the Hannover Medical School (No.

10856\_BO\_K\_2023). Written informed consent was obtained from all donors, parents, or guardians in the case of children.

# Peripheral blood mononuclear cell isolation

Peripheral blood mononuclear cells (PBMCs) were isolated by Ficoll-Paque density gradient centrifugation from EDTA blood samples collected at different time points after birth from the studied patient, as well as from nine uninfected healthy neonates (–3 days of age) and two neonates diagnosed with bacterial sepsis (2–3 days of age) at the AUF DER BULT Children's and Youth Hospital, Hannover, Germany. Additionally, PBMCs were isolated from an EDTA blood sample of a healthy adult for *in vitro* assays.

## FACS staining

Freshly isolated PBMCs were incubated for 20 min at room temperature with the following antibodies: anti-CD45 BUV395 (HI30; BD Bioscience), anti-CD3 BUV661 (UCHT1; BD Bioscience), anti-CD8 BUV805 (SK1; BD Bioscience), anti-CD4 BV570 (RPA-T4; BioLegend), anti-CD127 BV650 (A019D5; BioLegend), anti-CD25 PE-Fire700 (M-A250; BioLegend), anti-

γδ TCR PE (REA591; Miltenyi Biotec), anti-Vδ2 PerCPVio700 (REA771; Miltenyi Biotec), anti-Vγ9 FITC (REA470; Miltenyi Biotec), anti-Vδ1 VioGreen (REA173; Miltenyi Biotec), anti-CD45RA BV605 (HI100; BioLegend), anti-CD14 BB700 (ΜφP9; BD Bioscience), anti-CD16 BUV496 (3G8; BD Bioscience), anti-CD56 BUV564 (NCAM16.2; BD Bioscience), anti-CCR7 BV785 (G043H7; BioLegend), anti-CD19 Pe-Cy7 (HIB19; BD Bioscience), anti-IgD BV510 (IA6-2; BD Bioscience), and anti-CD27 Alexa Fluor (O323; BioLegend). Dead cells were detected using Zombi-NIR staining. After washing off excess antibodies, cells were acquired on an Aurora spectral flow cytometer (Cytek) using SpectroFlo v2.2.0 (Cytek). Flow cytometry data were analyzed in Flowjo 10.0 software.

# Cytokine measurement

Plasma cytokines were measured using the LEGENDplex $^{\mathrm{TM}}$  Human Essential Immune Response Panel (BioLegend) according to the manufacturer's instructions.

## CD3/Cd28 stimulation

Plates were coated overnight at 4°C with anti-CD3 antibody (BioLegend, #300438) at a final concentration of 4 µg/ml. Freshly isolated PBMCs  $(0.5 \times 10^6 \text{ cells/ml})$  were cultured in RPMI-1640 supplemented with 10% heat-inactivated FBS (Sigma), 1% GlutaMAX, 50 μM β-mercaptoethanol, 1% penicillin-streptomycin (all Gibco), and 100 U/ml IL-2. Anti-CD28 antibody was added to the coated wells at a final concentration of 1 µg/ml. Cells were incubated in a humidified CO2-incubator at 37°C for 48 h. After incubation cells were stained for 20 min at room temperature with fixable viability dye (Zombie NIR, BioLegend) and the following antibodies: anti-CD45 BUV395 (HI30; BD Bioscience), anti-CD14 BB700 (MφP9; BD Bioscience), anti-CD19 APC-Fire810 (HIB19; Biolegend), anti-CD3 BUV661 (UCHT1; BD Bioscience), anti-TCRγδ PE (REA591; Miltenyi Biotec), anti-CD4 APC (SK3; BD Bioscience), anti-CD8 BV510 (SK1; Biolegend), anti-CD69 BUV737 (FN50; FN50), anti-CD25 PE Fire 700 (M-A251; Biolegend), intracellular anti-TNF-α Alexa Fluor 700 (MAb11; BioLegend), intracellular anti-IFN-γ (B27; BioLegend). Acquisition was performed on an Aurora spectral flow cytometer (Cytek).

# Data availability statement

The datasets for this article are not publicly available due to concerns regarding participant/patient anonymity. Requests to access the datasets should be directed to the corresponding author.

## **Ethics statement**

The studies involving humans were approved by Institutional Review Board of the Hannover Medical School (no. 10856\_BO\_K\_2023). The studies were conducted in accordance with the local legislation and institutional requirements. Written informed consent for participation in this study was provided by the participants' legal guardians/next of kin. Written informed consent was obtained from the minor(s)' legal guardian/next of kin for the publication of any potentially identifiable images or data included in this article.

## **Author contributions**

XL-L: Writing - review & editing, Validation, Methodology, Formal analysis, Investigation, Writing - original draft, Conceptualization, Visualization. SR: Writing - review & editing, Conceptualization, Supervision, Writing - original draft, Funding acquisition. SH: Validation, Writing - review & editing, Methodology, Investigation. BA: Investigation, Writing - review & editing, Methodology. AB: Validation, Writing - review & editing, Supervision. LO: Writing - review & editing, Supervision, Validation. FG: Supervision, Writing - review & editing, Funding acquisition. CW: Writing - review & editing, Supervision, Validation. JB: Supervision, Writing - review & editing, Methodology. JW: Writing - review & editing, Supervision, Validation, Writing - original draft. MR: Conceptualization, Validation, Supervision, Investigation, Data curation, Funding acquisition, Writing - original draft, Writing - review & editing, Visualization.

# **Funding**

The author(s) declare that financial support was received for the research and/or publication of this article. The study received partial financial support from the non-profit Dr. August and Erika Appenrodt Foundation, which funds scientific projects aimed at promoting children's health.

# Acknowledgments

We thank the physicians and nurses of the Department of Neonatology and the laboratory staff at the Children's and Youth Hospital AUF DER BULT, as well as the scientific staff of the Institute of Immunology at the MHH, for their support and collaboration. Special thanks are extended to the families and the children for their participation, which contributed to the knowledge gained in this study.

## Conflict of interest

The authors declare that the research was conducted in the absence of any commercial or financial relationships that could be construed as a potential conflict of interest.

## Generative AI statement

The author(s) declare that no Generative AI was used in the creation of this manuscript.

Any alternative text (alt text) provided alongside figures in this article has been generated by Frontiers with the support of

artificial intelligence and reasonable efforts have been made to ensure accuracy, including review by the authors wherever possible. If you identify any issues, please contact us.

## Publisher's note

All claims expressed in this article are solely those of the authors and do not necessarily represent those of their affiliated organizations, or those of the publisher, the editors and the reviewers. Any product that may be evaluated in this article, or claim that may be made by its manufacturer, is not guaranteed or endorsed by the publisher.

## References

- 1. Dornan GL, Burke JE. Molecular mechanisms of human disease mediated by oncogenic and primary immunodeficiency mutations in class IA phosphoinositide 3-kinases. *Front Immunol.* (2018) 9:575. doi: 10.3389/fimmu.2018.00575
- 2. Engelman JA, Luo J, Cantley LC. The evolution of phosphatidylinositol 3-kinases as regulators of growth and metabolism. *Nat Rev Genet.* (2006) 7(8):606–19. doi: 10.1038/nrg1879
- 3. Madsen RR, Vanhaesebroeck B, Semple RK. Cancer-Associated PIK3CA mutations in overgrowth disorders. *Trends Mol Med.* (2018) 24(10):856–70. doi: 10.1016/j.molmed.2018.08.003
- 4. Rivière J-B, Mirzaa GM, O'Roak BJ, Beddaoui M, Alcantara D, Conway RL, et al. *de novo* germline and postzygotic mutations in AKT3, PIK3R2 and PIK3CA cause a spectrum of related megalencephaly syndromes. *Nat Genet.* (2012) 44(8):934–40. doi: 10.1038/ng.2331
- 5. Keppler-Noreuil KM, Rios JJ, Parker VER, Semple RK, Lindhurst MJ, Sapp JC, et al. PIK3CA -related overgrowth spectrum (PROS): diagnostic and testing eligibility criteria, differential diagnosis, and evaluation. *Am J Med Genet A*. (2015) 167(2):287–95. doi: 10.1002/ajmg.a.36836
- Mirzaa G, Timms AE, Conti V, Boyle EA, Girisha KM, Martin B, et al. PIK3CAassociated developmental disorders exhibit distinct classes of mutations with variable expression and tissue distribution. *JCI Insight*. (2016) 1(9):e87623. doi: 10.1172/jci. insight.87623
- 7. Mirzaa GM, Conway RL, Gripp KW, Lerman-Sagie T, Siegel DH, deVries LS, et al. Megalencephaly-capillary malformation (MCAP) and megalencephaly-polydactyly-polymicrogyria-hydrocephalus (MPPH) syndromes: two closely related disorders of brain overgrowth and abnormal brain and body morphogenesis. *Am J Med Genet A.* (2012) 158A(2):269–91. doi: 10.1002/ajmg.a.34402
- 8. Canaud G, Hammill AM, Adams D, Vikkula M, Keppler-Noreuil KM. A review of mechanisms of disease across PIK3CA-related disorders with vascular manifestations. *Orphanet J Rare Dis.* (2021) 16(1):306. doi: 10.1186/s13023-021-0129-8.
- 9. Cooley Coleman JA, Gass JM, Srikanth S, Pauly R, Ziats CA, Everman DB, et al. Clinical and functional characterization of germline PIK3CA variants in patients with PIK3CA -related overgrowth spectrum disorders. *Hum Mol Genet.* (2023) 32(9):1457–65. doi: 10.1093/hmg/ddac296

- 10. Yeung KS, Tso WWY, Ip JJK, Mak CCY, Leung GKC, Tsang MHY, et al. Identification of mutations in the PI3K-AKT-mTOR signalling pathway in patients with macrocephaly and developmental delay and/or autism. *Mol Autism.* (2017) 8(1):66. doi: 10.1186/s13229-017-0182-4
- 11. Mussa A, Leoni C, Iacoviello M, Carli D, Ranieri C, Pantaleo A, et al. Genotypes and phenotypes heterogeneity in PIK3CA-related overgrowth spectrum and overlapping conditions: 150 novel patients and systematic review of 1007 patients with PIK3CA pathogenetic variants. *J Med Genet.* (2023) 60(2):163–73. doi: 10. 1136/jmedgenet-2021-108093
- 12. Nunes-Santos CJ, Uzel G, Rosenzweig SD. Pl3K pathway defects leading to immunodeficiency and immune dysregulation. *J Allergy Clin Immunol.* (2019) 143(5):1676–87. doi: 10.1016/j.jaci.2019.03.017
- 13. Laval N, Kleiber N, Soucy J-F, Dubois J, Assaad M-A. Atypical presentation and evolution of necrotizing enterocolitis as a PIK3CA pathological variant. *Cureus*. (2024) 16(4):e59243. doi: 10.7759/cureus.59243
- 14. Venot Q, Blanc T, Rabia SH, Berteloot L, Ladraa S, Duong J-P, et al. Targeted therapy in patients with PIK3CA-related overgrowth syndrome. *Nature*. (2018) 558(7711):540–6. doi: 10.1038/s41586-018-0217-9
- 15. Parker VER, Keppler-Noreuil KM, Faivre L, Luu M, Oden NL, De Silva L, et al. Safety and efficacy of low-dose sirolimus in the PIK3CA-related overgrowth spectrum. *Genet Med.* (2019) 21(5):1189–98. doi: 10.1038/s41436-018-0297-9
- 16. Forde K, Resta N, Ranieri C, Rea D, Kubassova O, Hinton M, et al. Clinical experience with the AKT1 inhibitor miransertib in two children with PIK3CA-related overgrowth syndrome. *Orphanet J Rare Dis.* (2021) 16(1):109. doi: 10.1186/s13023-021-01745-0
- 17. Okkenhaug K. Signaling by the phosphoinositide 3-kinase family in immune cells. *Annu Rev Immunol.* (2013) 31(1):675–704. doi: 10.1146/annurev-immunol-032712-095946
- 18. Richards S, Aziz N, Bale S, Bick D, Das S, Gastier-Foster J, et al. Standards and guidelines for the interpretation of sequence variants: a joint consensus recommendation of the American college of medical genetics and genomics dhe association for molecular pathology. *Genet Med.* (2015) 17(5):405–24. doi: 10.1038/gim.2015.30